Jasmonic Acid Is Required for Plant Acclimation to a Combination of High Light and Heat Stress[1][OPEN]

Damián Balfagón,[a] Soham Sengupta,[b] Aurelio Gómez-Cadenas,[a] Felix B. Fritschi,[c] Rajeev K. Azad,[b] Ron Mittler,[c,2] and Sara I. Zandalinas[c,2,3]

[a]Departamento de Ciencias Agrarias y del Medio Natural, Universitat Jaume I, Castello de la Plana, 12071 Spain
[b]Department of Biological Sciences, College of Science, University of North Texas, Denton, Texas 76203
[c]Bond Life Sciences Center, Interdisciplinary Plant Group, and Division of Plant Sciences, College of Agriculture, Food and Natural Resources, University of Missouri, Columbia, Missouri 65211

ORCID IDs: 0000-0003-1924-8412 (D.B.); 0000-0002-5013-1506 (S.S.); 0000-0002-4598-2664 (A.G.-C.); 0000-0003-0825-6855 (F.B.F.); 0000-0003-3192-7450 (R.M.); 0000-0002-1256-9371 (S.I.Z.).

In the field, plants experience high light (HL) intensities that are often accompanied by elevated temperatures. Such conditions are a serious threat to agriculture production, because photosynthesis is highly sensitive to both HL intensities and high-temperature stress. One of the potential cellular targets of HL and heat stress (HS) combination is PSII because its degree of photoinhibition depends on the balance between the rate of PSII damage (induced by light stress), and the rate of PSII repair (impaired under HS). Here, we studied the responses of Arabidopsis (*Arabidopsis thaliana*) plants to a combination of HL and HS (HL+HS) conditions. Combined HL+HS was accompanied by irreversible damage to PSII, decreased D1 (PsbA) protein levels, and an enhanced transcriptional response indicative of PSII repair activation. We further identified several unique aspects of this stress combination that included enhanced accumulation of jasmonic acid (JA) and JA-Ile, elevated expression of over 2,200 different transcripts that are unique to the stress combination (including many that are JA-associated), and distinctive structural changes to chloroplasts. A mutant deficient in JA biosynthesis (allene oxide synthase) displayed enhanced sensitivity to combined HL+HS and further analysis revealed that JA is required for regulating several transcriptional responses unique to the stress combination. Our study reveals that JA plays an important role in the acclimation of plants to a combination of HL+HS.

The majority of plants growing under direct sunlight routinely encounter light intensities that exceed their photosynthetic capacity (Ort, 2001). An additional environmental parameter that may accompany high light (HL) intensities is heat stress (HS). In the past several years, the frequency of extreme weather events combining HL and high-temperature conditions has increased dramatically, especially in the summer at midday, when temperatures often rise to 30°C to 40°C and light intensity reaches 2,000 μmol m^{-2} s^{-1} (Yamamoto et al., 2008; Suzuki et al., 2014). HL intensity and high temperatures are both abiotic conditions that can drastically impact the photosynthetic machinery and limit the growth and development of plants. During HL stress, the reaction centers become saturated and the excess excitation energy can become harmful because it can irreversibly damage PSII (Murata et al., 2007; Ruban, 2009, 2015). This damaging scenario leads to photoinhibition—a sustained decline in photosynthetic efficiency caused by the imbalance between the rate of photodamage to PSII and the rate of PSII repair (Nishiyama et al., 2006; Murata et al., 2007). In addition to HL stress, HS can compromise PSII electron transport due to the increase in fluidity of the thylakoid membranes, which causes dislodging of PSII light harvesting complexes (LHC) and decreased integrity of PSII (Mathur et al., 2014). HS can also impair the repair process of PSII, exacerbating the effects of HL stress (Takahashi and Murata, 2008; Dogra et al., 2019). Moreover, HL intensities and HS may each induce the production of reactive oxygen species (ROS) via different mechanisms (Murata et al., 2007; Pospíšil, 2016),

[1]This work was supported by funding from the National Science Foundation (grant nos. IOS-1353886, MCB-1936590, and IOS-1932639), the Bond Life Sciences Early Concept Grant, the University of Missouri, the Ministerio de Ciencia, Innovación y Universidades (grant no. AGL2016-76574-R), and the "Fundación Balaguer Gonel Hermanos" (to D.B.).

[2]Senior authors.
[3]Author for contact: izquierdozandalins@missouri.edu.
The author responsible for distribution of materials integral to the findings presented in this article in accordance with the policy described in the Instructions for Authors (www.plantphysiol.org) is: Sara I. Zandalinas (izquierdozandalins@missouri.edu).

D.B. and S.I.Z. performed the research; S.I.Z., R.M., F.B.F., and A.G.-C. designed and supervised the research; R.M. and A.G.-C. provided laboratory infrastructure and funding; S.S. and R.K.A. performed the transcriptomic bioinformatics analysis; D.B., S.I.Z., and R.M. wrote the article and prepared figures; all authors read and approved the final version of the article.
[OPEN]Articles can be viewed without a subscription.
www.plantphysiol.org/cgi/doi/10.1104/pp.19.00956

potentially leading to a distinct ROS signature when the two stresses are combined (Choudhury et al., 2017).

In plants, PSII contains more than 20 subunits including four major core subunits termed "D1" (PsbA), "D2" (PsbD), "CP43" (PsbC), and "CP47" (PsbB; Allen et al., 2011). Among them, the D1 protein is the main site susceptible to damage by HS or HL (Murata et al., 2007; Yamamoto et al., 2008; Su et al., 2014). Plants evolved several different protective systems to survive under unfavorable light conditions (Szymańska et al., 2017). After PSII inactivation by light, its activity can be restored by a highly coordinated multistep repair system that involves degradation of damaged D1, de novo D1 synthesis, and PSII reassembly (Lu, 2016). This repair cycle includes the disassembly of the PSII–LHCII supercomplex and the PSII core dimer in grana stacks, followed by lateral migration of the PSII core monomer to stroma-exposed thylakoid membranes, dephosphorylation, partial disassembly of the PSII core monomer, and degradation of photodamaged D1. Finally, de novo synthesis and reassembly of D1, reincorporation of CP43, migration of the PSII core monomer back to grana stacks, dimerization into PSII core dimers, and reformation of PSII–LHCII supercomplexes occurs (for review, see Lu, 2016). More than 60 auxiliary proteins, enzymes, and components of thylakoid protein trafficking/targeting systems are directly or indirectly involved in the PSII repair cycle (Baena-González and Aro, 2002; Lu, 2016). For example, FtsH proteases are involved in the degradation of photodamaged D1. It has been reported that *var2-2* plants, deficient in FtsH, are much more susceptible to light-induced PSII photoinhibition than wild-type plants (Bailey et al., 2002), suggesting that impaired PSII repair could lead to an inability to acclimate to HL intensity.

Phytohormones play important roles in regulating responses to a wide variety of biotic and abiotic stresses. Among them, jasmonates have been traditionally associated with defense responses against herbivores, necrotrophic pathogens, nematodes, and other biotic threats. In addition, jasmonic acid (JA) and its conjugate form, JA-Ile, have been implicated in responses to abiotic challenges such as UV, osmotic stress, salinity, cold, heat, and heavy metal stresses (for review, see Wasternack and Hause, 2013; Dar et al., 2015; Kazan, 2015). A study of the ultra-fast transcriptomic response of Arabidopsis to light stress revealed that ~12% of transcripts that accumulated within seconds of light stress application were JA-response transcripts (Suzuki et al., 2015), suggesting a possible role for this phytohormone in rapid responses to HL-intensity stress.

Because combined light and HS occurs during the summer season in many of the areas used for crop production worldwide, we studied the effect of this stress combination on the model plant Arabidopsis (*Arabidopsis thaliana*). Here, we uncover the unique transcriptomic, physiological, and hormonal responses of Arabidopsis plants to a combination of HL and HS (HL+HS). Because both stresses impact PSII performance, albeit in different ways, we hypothesized that the stress combination would have a severe effect on PSII performance, higher than that of the individual stresses. Here we show that combined HS and HL has a detrimental effect on plants and that this stress combination has unique physiological and molecular characteristics, including a decreased ability to repair PSII. We further reveal that JA plays a key role in the response of plants to this stress combination. By contrast, abscisic acid (ABA) and salicylic acid (SA) play much lesser roles. Our findings reveal that the response of Arabidopsis plants to a combination of HL+HS is unique, and might require dedicated breeding efforts to overcome under field conditions.

RESULTS

Acclimation of Arabidopsis Plants to HL, HS, and a Combination of HL+HS

To study the responses to HL, HS, and their combination, we subjected wild-type Arabidopsis plants (Columbia [Col]) to a light intensity of 600 μmol m^{-2} s^{-1} HL, a temperature of 42°C HS, or to a light intensity of 600 μmol m^{-2} s^{-1} combined with a temperature of 42°C (HL+HS) for 7 h (Fig. 1A; Supplemental Fig. S1). By contrast, control (CT) plants were maintained under 50 μmol m^{-2} s^{-1} at 23°C. PSII performance in terms of quantum yield of PSII (Φ_{PSII}) and maximal efficiency of PSII (F_v/F_m) were determined in Col plants subjected to HL, HS, and HL+HS (Fig. 1, B and C). Φ_{PSII} and F_v/F_m values significantly decreased after the application of HL, and more dramatically after the application of HL+HS, compared to CT values. By contrast, HS did not significantly affect PSII activity (Fig. 1, B and C, top). To examine the ability of plants to recover from stress, we measured Φ_{PSII} and F_v/F_m 24 h after the stress treatments (Fig. 1, B and C, bottom; Supplemental Fig. S1). As shown in Figure 1, B and C, Φ_{PSII} and F_v/F_m values of plants subjected to HL returned to CT values whereas those of plants subjected to the stress combination remained significantly lower compared to CT plants. These findings suggest that PSII function could not be completely recovered 24 h after exposure to HL+HS conditions. The leaf damage index (LDI) demonstrated that ~6% of leaves showed damage in response to HL, whereas all leaves looked healthy in plants subjected to HS (Fig. 1, A and D). By contrast, Col plants subjected to the stress combination showed a higher number of affected leaves (35% dead and 38% damaged; Fig. 1, A and D). In addition, whereas all plants survived the application of HL or HS, the combination of HL and HS significantly decreased survival rate to 75% (Fig. 1, A and D).

Stomatal Responses of Arabidopsis Plants to HL, HS, and HL+HS Stress Combination

Because stomata were previously shown to close during light stress (Devireddy et al., 2018), but open during HS (Rizhsky et al., 2004; Teskey et al., 2015;

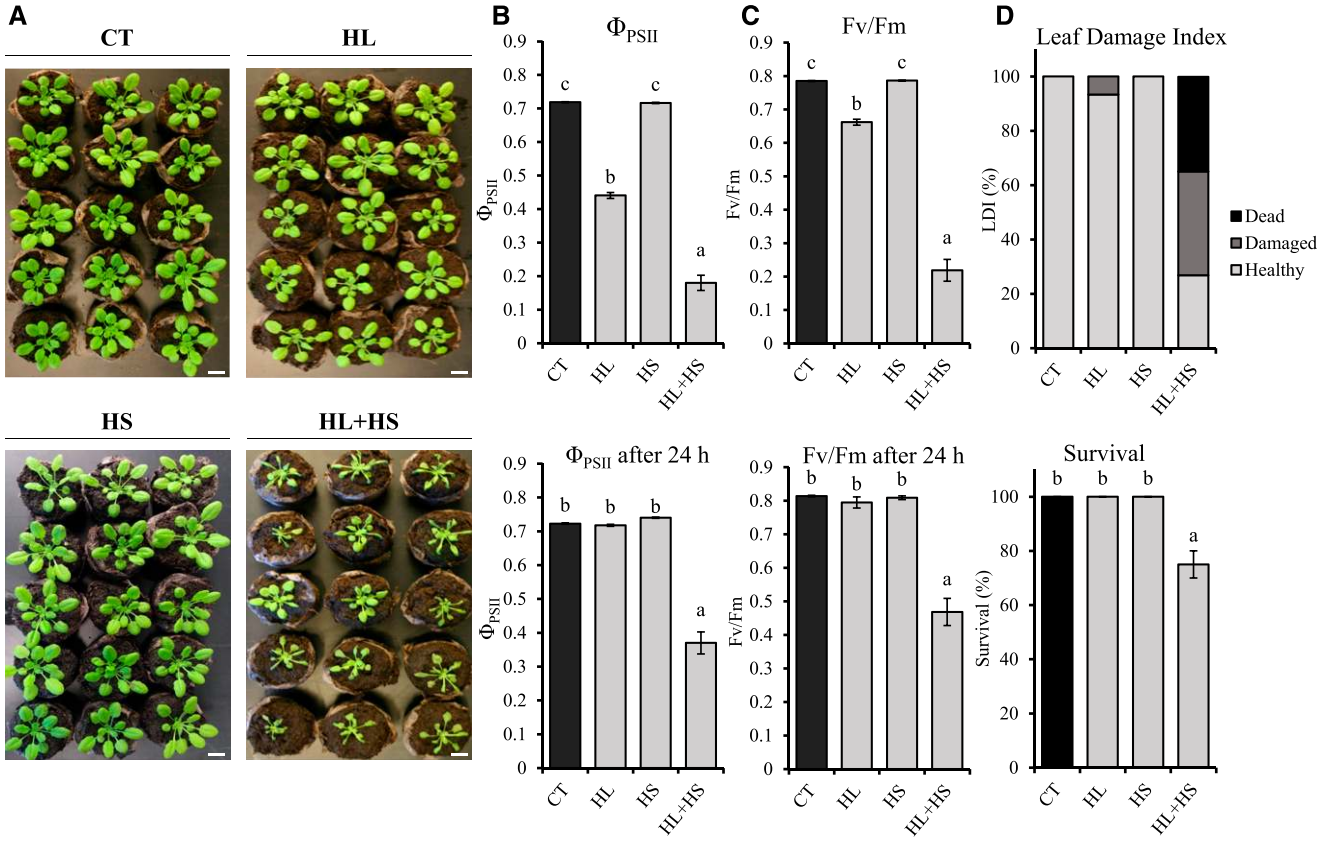

Figure 1. A combination of HL+HS is detrimental to plants. A, Representative images of Col plants subjected to HL, HS, and combined HL+HS. Scale bar = 1 cm. B, Φ_{PSII} immediately after the application of each stress (top) and 24 h after recovery from the stress treatments (bottom). C, F_v/F_m immediately after the application of each stress (top) and 24 h after recovery from the stress treatments (bottom). D, LDI of Col plants after the stress treatments (top) and survival of plants subjected to the different stresses (bottom). Error bars represent SD ($n = 30$). Values statistically different at $P < 0.05$ are denoted with different letters.

Zandalinas et al., 2016a; Urban et al., 2017), suggesting a potential conflict in the response of plants to HL+HS, we tested the effect of HL+HS on stomatal aperture (Fig. 2). Whereas HL induced a decrease in stomatal aperture (23% compared to CT), both HS and HL+HS induced stomatal opening. Leaf temperature increased in plants subjected to HL by ~4°C compared to leaves of CT plants. By contrast, the leaf temperature of HS plants was higher, ~10°C higher than CT, whereas combined HL+HS caused leaf temperature to increase to ~10°C to 12°C higher than CT. Consequently, leaf relative water content (RWC) significantly decreased primarily in plants subjected to HS or HL+HS compared to CT values (Fig. 2). These results demonstrate that from the standpoint of signal transduction mechanisms regulating stomatal conductance, the combination of HL+HS is more similar to HS than to HL.

Transcriptomic Responses of Arabidopsis Plants to HL, HS, and HL+HS Stress Combination

A transcriptomic (RNA sequencing [RNA-seq]) analysis of Col plants subjected to HL, HS, and HL+HS conditions revealed that the steady-state level of 3,942, 5,304, and 6,314 transcripts was significantly enhanced in response to HL, HS, and HL+HS, respectively (Fig. 3A; Supplemental Tables S1–S6), and a high proportion of these transcripts was associated with hormone and ROS responses (Table 1; Suzuki et al., 2015; Zandalinas et al., 2019a). In addition, the steady-state level of 3,670, 4,994, and 5,678 transcripts was significantly decreased in response to HL, HS, and HL+HS, respectively (Fig. 3A; Supplemental Tables S4–S6). Of the 6,314 transcripts significantly elevated in response to HL+HS, 2,125 transcripts (34%) were common with HL-induced transcripts, 3,166 transcripts (50%) were common with HS-induced transcripts, and 2,239 transcripts (36%) were found to be specifically upregulated by the stress combination. These results suggest that a considerable proportion of the transcriptomic changes in plants subjected to HL+HS is specific for the stress combination. According to gene ontology (GO) term enrichment analysis (Fig. 3B; Supplemental Fig. S2), HL+HS-specific transcripts are involved in different biological processes including oxidation-reduction processes, protein transport, protein catabolic processes, or photosynthesis, as well as related to

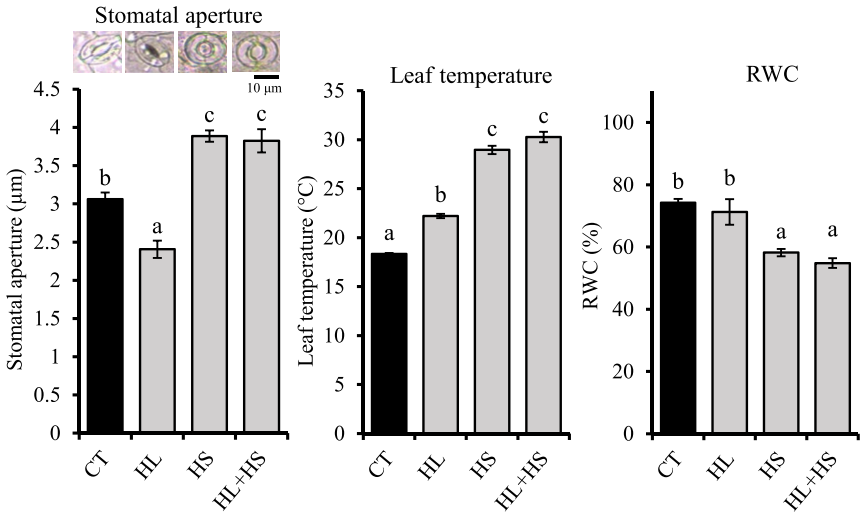

Figure 2. Combined HL+HS causes a heat-like stomatal response. Stomatal aperture (left), surface leaf temperature (middle), and leaf RWC (right) of Col plants subjected to HL, HS, and combined HL+HS. Error bars represent SD (n = 600 for stomatal aperture; n = 50 for leaf temperature and RWC). Values statistically different at $P < 0.05$ are denoted with different letters. Representative stomatal images are shown on the left. Scale bar in stomatal images = 10 μm.

responses to cadmium, salt stress, or involved in the tricarboxylic acid cycle (Fig. 3B).

The expression of genes encoding selected transcriptional regulators involved in plant responses to different stresses, such as Heat Shock Factors (HSFs), APETALA2 (AP2)/ethylene-responsive element binding proteins (EREBPs), and MYBs, revealed a differential expression pattern in plants subjected to HL, HS, and HL+HS compared to CT (Fig. 4). As shown in Figure 4, some HSFs displayed an additive manner of expression, with *HSFA2*, *HSFA7A*, *HSFB1*, *HSFB2A*, and *HSFB2B* showing the highest expression values in response to HL+HS. By contrast, other HSFs were specifically upregulated in response to HS (*HSFA6B*) or HL (*HSFA1D*; Fig. 4A). Interestingly, no HSF was found to be uniquely expressed during the HL+HS response. In contrast to HSFs, genes encoding several AP2/EREBP transcription factors were upregulated specifically in response to HL+HS (Fig. 4B). These included *ERF109*, *ERF88*, *DREB1D*, *ERF25*, *ERF57*, *ERF4*, and *ERF99* (Fig. 4B). A similar pattern with the steady-state level of several transcriptional regulators enhanced specifically during HL+HS was also found for the MYB family (Fig. 4C). For instance, *MYB50*, *MYB15*, *MYB35*, *MYB62*, *MYB86*, *MYB77*, *MYB17*, and *MYB23* were specifically upregulated in response to HL+HS,

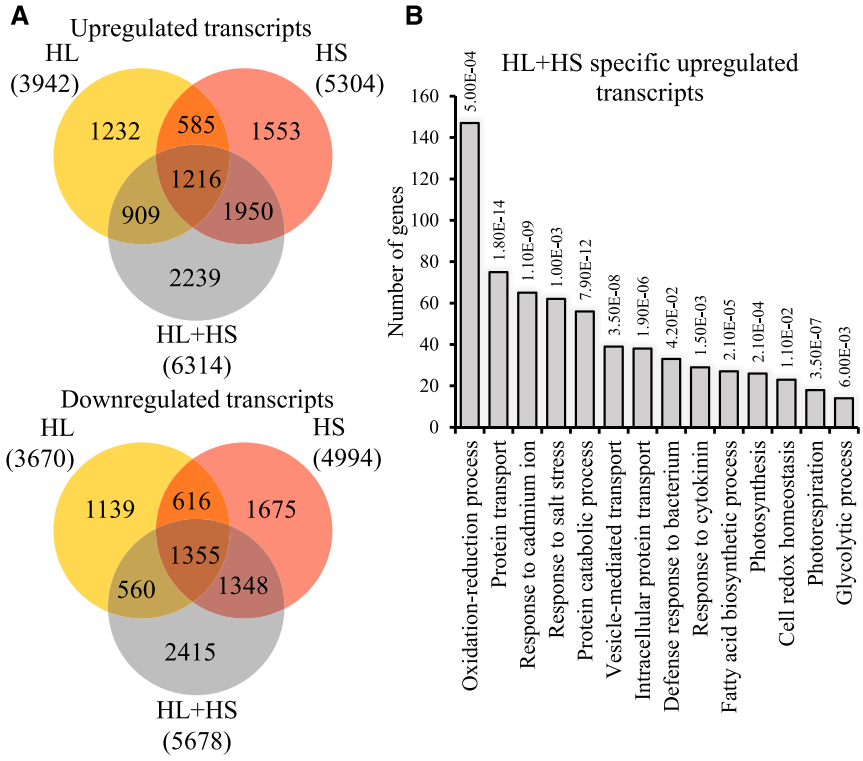

Figure 3. Combined HL+HS is accompanied by a unique transcriptomic response. A, Venn diagrams showing the overlap among the upregulated (top) and downregulated (bottom) transcripts in each of the different stress treatments (HL, HS, and combined HL+HS). B, GO annotation of transcripts specifically upregulated in leaves of Arabidopsis in response to HL+HS (numbers above each bar represent P value for statistical significance).

Table 1. *Representation of hormone- and ROS-response transcripts in the transcriptomic response of plants subjected to HL, HS, and the combination of HL+HS*

Hormone/ROS	HL	HS	HL+HS
Abscisic acid (1,460)	220 (15.07%)	472 (32.33%)	554 (37.94%)
1-Aminocyclopropane-1-carboxylic acid (175)	19 (10.86%)	30 (17.14%)	36 (20.57%)
Brassinolide (276)	19 (6.88%)	31 (11.23%)	60 (21.74%)
Cytokinin (355)	154 (43.38%)	121 (34.08%)	110 (30.98%)
Gibberellin (43)	6 (13.95%)	9 (20.93%)	8 (18.60%)
Indole-3-acetic acid (436)	43 (9.86%)	70 (16.05%)	90 (20.64%)
Methyl jasmonate (3,877)	611 (15.76%)	689 (17.77%)	829 (21.38%)
Salicylic acid (217)	21 (9.67%)	23 (10.60%)	37 (17.05%)
H_2O_2 (956)	166 (17.36%)	229 (23.95%)	354 (37.03%)
O_2^- (287)	1 (0.35%)	2 (0.69%)	3 (1.04%)
$^1O_2$ (297)	47 (15.82%)	70 (23.57%)	80 (26.94%)

whereas *MYB90*, *MYB11*, *MYB114*, *MYB113*, and *MYB97* were specifically upregulated in response to HL or HS (Fig. 4C). These findings highlight particular transcriptional regulators and their related families as potential breeding targets for future efforts to develop plants with enhanced tolerance to HL+HS combination. In addition, they reveal the complexity underlying plant acclimation to this stress combination.

Impact of HL+HS Combination on PSII and Different Chloroplast Structures

Because HL and HS negatively impact the photosynthetic machinery (Mathur et al., 2014; Ruban, 2015), and one of the major impacts of HL+HS appears to be PSII (Fig. 1), we analyzed the expression of transcripts encoding photosynthetic proteins in our RNA-Seq data set (Fig. 3). As shown in Figure 5A, transcripts encoding PSII proteins (PsbC, PsbA, PsbB, PsbE, PsbF, PsbH, or PsbZ), PSI (PsaA, PsaK, PsaC, or PsaH), proteins of the cytochrome b_6f complex (PetB and PetC), and proteins involved in photosynthetic electron transport (PetE and PetF) were upregulated in response to HL+HS (with some upregulated in response to HL or HS as well). In addition, HL or the HL+HS combination enhanced the expression of several transcripts encoding antenna proteins such as Lhcb4.3, Lhcb7, and Lhca5 (Fig. 5A). Because the D1 protein of PSII (encoded by PsbA) is considered to be highly sensitive to photodamage (Edelman and Mattoo, 2008), we further analyzed the levels of D1 under the different stresses (Fig. 5B; Supplemental Fig. S3A), as well as the expression of transcripts that encode proteins involved in the PSII repair cycle (Lu, 2016; Fig. 5C). Whereas HS and HL significantly increased the accumulation of D1 with respect to CT plants, plants subjected to HL+HS displayed reduced levels of this protein (Fig. 5B; Supplemental Fig. S3A). In addition, many transcripts encoding proteins involved in D1 degradation (FtsH1, FtsH5, FtsH6, and FtsH8), its repair (CYP20-3 and PSB27), and the reassembly of PSII (CYP20-3, LQY1, PBF1, HCF136, and PSB33; Järvi et al., 2015; Lu, 2016), were upregulated in response to HL+HS, suggesting that the PSII repair cycle is activated under this stress combination (Fig. 5C). Our findings suggest that the D1 protein of PSII is particularly sensitive to the combination of HL+HS, and that plants subjected to this stress combination are attempting to repair this protein. Nevertheless, as shown in Figure 1, the combination of HL+HS results in an overall decline in PSII activity during the stress combination.

To determine the degree of structural changes to chloroplasts resulting from the stress combination, we conducted transmission electron microscopy (TEM) analysis of leaf samples from plants subjected to the different treatments. As shown in Figure 6, HL-induced structural changes to chloroplasts included a decrease in the number of starch granules and enhanced stacking of thylakoids (number of thylakoid membranes per micrometer; Fig. 6B). By contrast, chloroplasts of HS-treated plants appeared to contain a higher number of starch granules, as well as reduced granal stacking (Fig. 6B). Interestingly, compared to CTs, HL+HS-induced structural changes included an increased number of starch granules, of which ~75% appeared highly distorted, as well as fewer thylakoids per μm (Fig. 6). Plant subjected to HL+HS therefore displayed unique structural features of distorted starch granules, as well as reduced granal stacking. These features suggest that the impact of HL+HS on chloroplast structure and metabolism is unique and should be addressed in future studies.

Accumulation of H_2O_2, ABA, SA, JA, JA-Ile, and 12-Oxo-Phytodienoic Acid in Arabidopsis Plants Subjected to HL+HS Combination

A large number of phytohormones and ROS are involved in the responses of plants to different abiotic stresses and their combinations (Peleg and Blumwald, 2011; Choudhury et al., 2017). To further dissect the response of plants to a combination of HL+HS, we measured the levels of H_2O_2, ABA, SA, JA, JA-Ile, and 12-oxo-phytodienoic acid (OPDA) in all treatments. As shown in Figure 7, H_2O_2 and ABA content significantly increased in Arabidopsis wild-type Col leaves in response

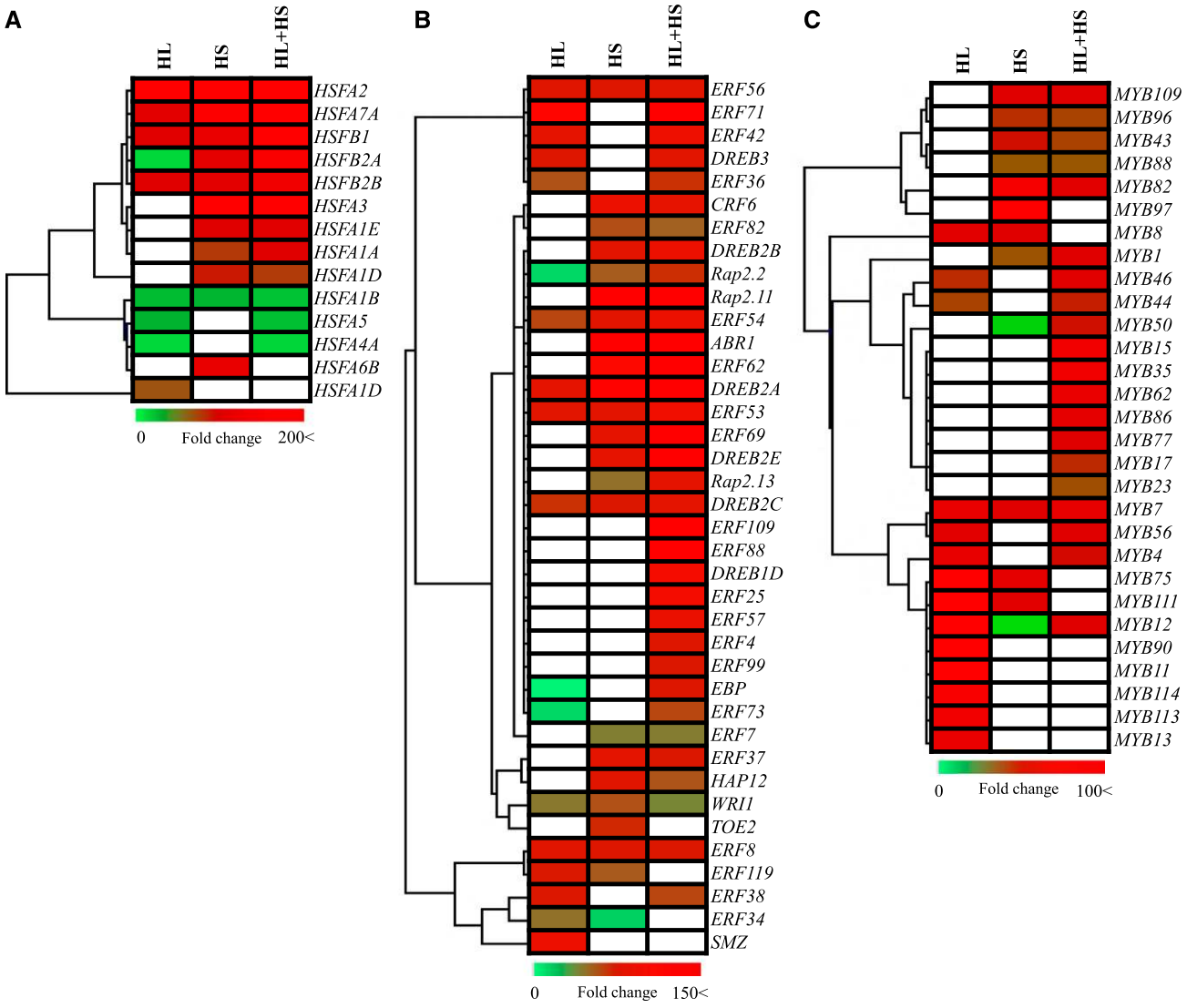

Figure 4. Differential expression of transcriptional regulators during the stress combination. Heat maps showing the response of different transcriptional regulators in HL, HS, and combined HL+HS conditions (relative to CT). A, HSF family. B, AP2/EREBP family. C, MYB family.

to HS and the combination of HL+HS (Fig. 7, A and B). In contrast, SA levels decreased in response to all stress treatments (Fig. 7C). Interestingly, compared to CT, HL, and HS treatments, the levels of JA and its conjugate JA-Ile dramatically increased in response to the stress combination. In addition, levels of the JA precursor OPDA (Stenzel et al., 2003) increased in response to HL, HS, and HL+HS (Fig. 7D). These results suggest that jasmonates, in particular JA and JA-Ile, are playing an important role in the acclimation of plants to this stress combination.

Characterizing the Response of JA-Deficient (*aos*) Plants to HL+HS Stress Combination

To further dissect the role of JA in the response of plants to the HL+HS combination, we compared our transcriptomic data with previous reports that identified transcripts that respond to changes in jasmonate levels (Taki et al., 2005; Suzuki et al., 2015; Hickman et al., 2017). We found that out of the 6,314 transcripts that were upregulated in response to HL+HS, 822 transcripts (13%) were associated with jasmonate responses (Fig. 8A; Table 1; Supplemental Fig. S4). In addition, as shown in Figure 8A, the expression of genes encoding many transcriptional regulators that were shown to respond to jasmonates (Taki et al., 2005; Suzuki et al., 2015; Hickman et al., 2017) was upregulated in response to HL+HS and some of these were specific for the stress combination (including *bZIP3*, *BHLH114*, *BHLH137*, *WRKY8*, *WRKY57*, and *WRKY18*). In addition, the expression of many transcripts involved in JA biosynthesis was upregulated in plants subjected to the stress combination (Supplemental Fig.

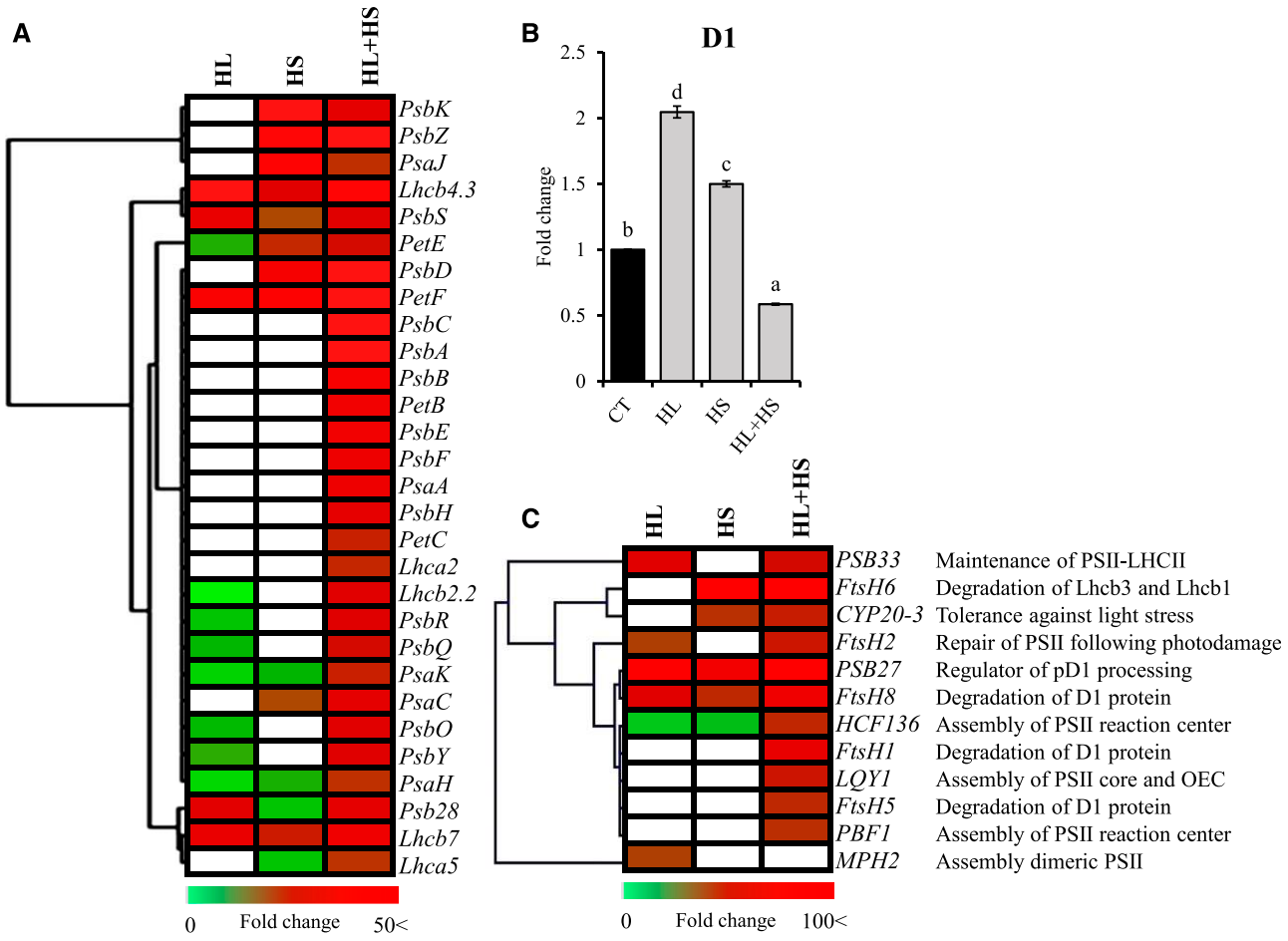

Figure 5. Enhanced expression of transcripts encoding PSII and PSII repair proteins during combined HL+HS is accompanied by a decrease in D1. A, Heat map showing changes in expression of transcripts encoding proteins of the photosynthetic apparatus in Col leaves in response to HL, HS, and the combination of HL+HS. B, Accumulation of D1 proteins in response to each stress condition. Error bars represent SD ($n = 3$). Values statistically different at $P < 0.05$ are denoted with different letters. C, Heat map showing changes in the expression of transcripts encoding proteins involved in the D1 turnover in Col leaves in response to each stress.

S4). These findings suggest that JA could be mediating some of the HL+HS-specific transcriptional responses identified in Figure 3.

To further study the role of JA in the response of plants to HL+HS combination, we analyzed the responses of the highly studied JA-deficient mutant *aos* (Park et al., 2002; Chehab et al., 2012; Hu et al., 2013; Gasperini et al., 2015) to HL, HS, and HL+HS (Fig. 8, B–D; Supplemental Fig. S5). As shown in Figure 8C, compared to CT, Φ_{PSII} and F_v/F_m values of *aos* mutants significantly decreased in response to HL and more markedly in response to HL+HS. In addition, whereas all *aos* plants survived the individual HL or HS stresses, the survival rate of *aos* plants subjected to a combination of HL and HS decreased to ~49% (Fig. 8D, top). Furthermore, when analyzing leaf damage (using the LDI) in *aos* plants subjected to the different stresses, we found that ~33% of leaves were damaged by HL whereas signs of stress were not apparent in *aos* plants subjected to HS. By contrast, HL+HS negatively influenced leaf appearance, with 60% of leaves dead, 30% of leaves damaged, and only 10% of leaves healthy (Fig. 8D, bottom). Compared to Col plants, *aos* mutants were therefore more sensitive to the stress combination (displaying a significantly reduced survival rate and LDI; Fig. 8, B and D; Table 2). By contrast to the *aos* mutant, mutants deficient in ABA (*aba2*) or SA (*sid2*) did not display higher sensitivity to the HL+HS stress combination compared to wild-type Col plants (Table 2; Supplemental Figs. S6 and S7).

To determine whether the differences in survival of Col and *aos* plants subjected to the stress combination (Table 2) were related to JA-dependent changes in transcript expression, we analyzed the expression of genes encoding different jasmonate-responsive transcriptional regulators (*ZAT6*, *ZAT10*, and *MYB15*; Taki et al., 2005; Suzuki et al., 2015; Hickman et al., 2017), as well as the ROS-scavengers *APX1* and *APX2*, in Col and *aos* plants subjected to the different stress treatments (Fig. 8E). Whereas *ZAT6* and *MYB15* were previously reported to respond to MeJA (Suzuki et al., 2015; Hickman et al., 2017), *ZAT10* expression was associated

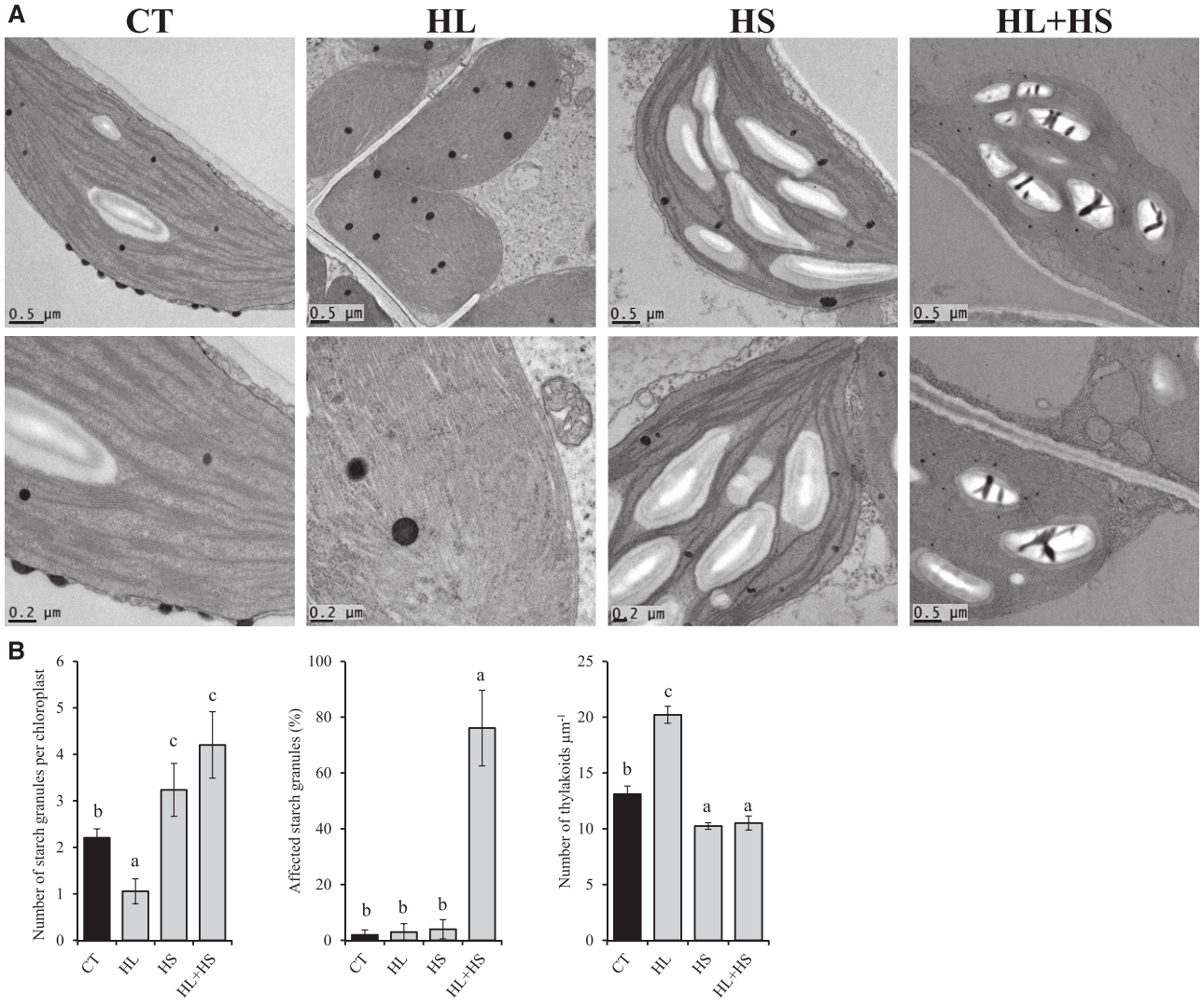

Figure 6. Unique structural features of chloroplasts from plants subjected to HL, HS, and combined HL+HS. A, Representative TEM images of chloroplasts of Col plants subjected to the different stresses. Images were taken at different magnification levels. Scale bar = 0.5 or 0.2 μm (as labeled in each image). B, Quantification bar graphs showing structural changes to chloroplasts of plants subjected to the different stresses. At least 100 images, each containing two to four chloroplasts from at least three plants from each treatment, were analyzed. Error bars represent SD. Values statistically different at $P < 0.05$ are denoted with different letters.

with OPDA (Taki et al., 2005) as well as ROS (Willems et al., 2016) and ABA responses (Song et al., 2016). In *aos* plants that do not accumulate OPDA, JA, and JA-Ile (Chehab et al., 2011), the expression of *ZAT6*, *ZAT10*, *APX1*, and *APX2* was significantly reduced compared to wild-type plants in response to the combination of HL+HS (Fig. 8E), suggesting that JA-dependent responses could be key for plant tolerance to the combination of HL+HS.

DISCUSSION

Plants growing within their natural habitat are routinely subjected to a combination of different environmental stresses that could adversely impact their growth and productivity (Mittler, 2006). The ability to sense and respond to these adverse conditions is therefore crucial for plants. This study focused on the ability of plants to acclimate to a combination of HL and HS. The frequency of this stress combination has increased during the last several years, affecting the photosynthetic performance of plants (Yamamoto et al., 2008; Suzuki et al., 2014). Previous reports analyzed some aspects of the response of different plant species to a combination of HL and HS. Lipidomics analysis in tomato (*Solanum lycopersicum*) identified lipophilic antioxidant molecules that could potentially contribute to the protection of PSII against photodamage and facilitate enhanced tolerance of combined HL+HS

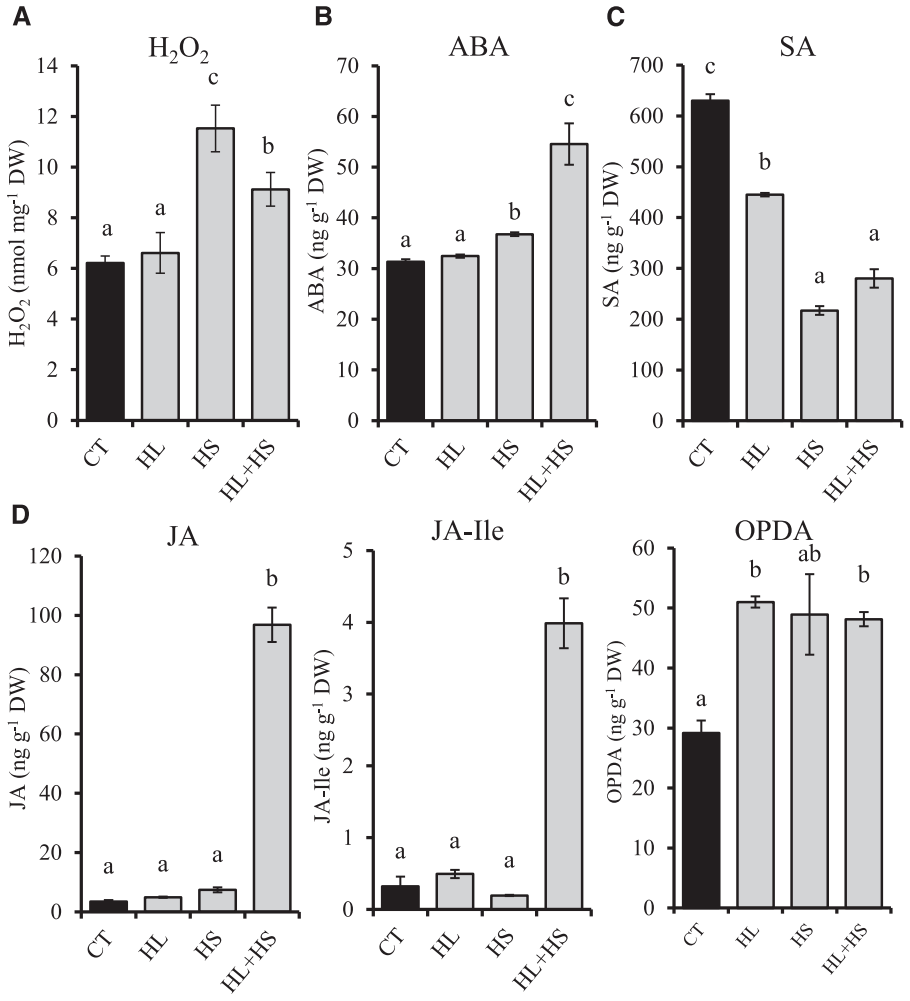

Figure 7. Levels of H_2O_2, ABA, SA, JA, JA-Ile, and OPDA in Col plants subjected to HL, HS, and combined HL+HS. A, H_2O_2. B, ABA. C, SA. D, JA, JA-Ile, and OPDA. Error bars represent SD ($n = 15$). Values statistically different at $P < 0.05$ are denoted with different letters.

(Spicher et al., 2017). In addition, studies in sunflower (*Helianthus annuus*) identified responses specific to combined HL+HS involving the upregulation of transcripts associated with energy metabolism, protein synthesis, cell wall activity, and signal transduction components (Hewezi et al., 2008). However, to our knowledge, a comprehensive physiological, hormonal, and transcriptomic analysis of this stress combination has not been conducted in the model plant Arabidopsis to date.

Our study of the stomatal responses of plants subjected to HL, HS, and HL+HS combination (Fig. 2) suggest that during the stress combination the effect of high temperature, i.e. opening of stomata to increase transpiration and cool the leaf (Rizhsky et al., 2004; Zandalinas et al., 2016a), prevailed over the effect of HL, i.e. reducing stomatal aperture (Devireddy et al., 2018). Light-stress–induced stomatal closure, potentially to prevent water loss (Fig. 2), could limit CO_2 uptake and therefore energy supply (Flexas et al., 2002), possibly leading to a decreased number of starch granules in chloroplasts (Fig. 6). By contrast, HS and HL+HS enhanced stomatal aperture, to decrease leaf temperature via transpiration (Rizhsky et al., 2002, 2004; Zandalinas et al., 2016a), potentially leading to a reduced RWC in these plants (Fig. 2). The appearance of more starch granules in the chloroplasts of HS- and HL+HS-treated plants (Fig. 6) could indicate an increased rate of CO_2 fixation due to stomatal opening (Fig. 2). Interestingly, under HL+HS treatment, starch granules appeared highly distorted (Fig. 6). The reason for this distortion could be attributed to an altered amylose/amylopectin ratio during the stress combination, and/or a possible rupture of the plastidial envelope during stress combination, allowing access for starch-degrading enzyme (Bondada and Syvertsen, 2005). Further studies are needed to unravel the role of different metabolic pathways during a combination of HL and HS and their effect on chloroplast structures. It is nevertheless important to note that, in contrast to a combination of drought and HS, in which the effect of drought prevailed over the effect of heat on stomatal conductance (i.e. stomata remained closed during the stress combination; Rizhsky et al., 2002, 2004), in this study the effect of HS prevailed over HL (i.e. stomata remained open; Fig. 2). Further studies addressing the different mechanisms modulating stomatal conductance during different stress combinations may reveal the

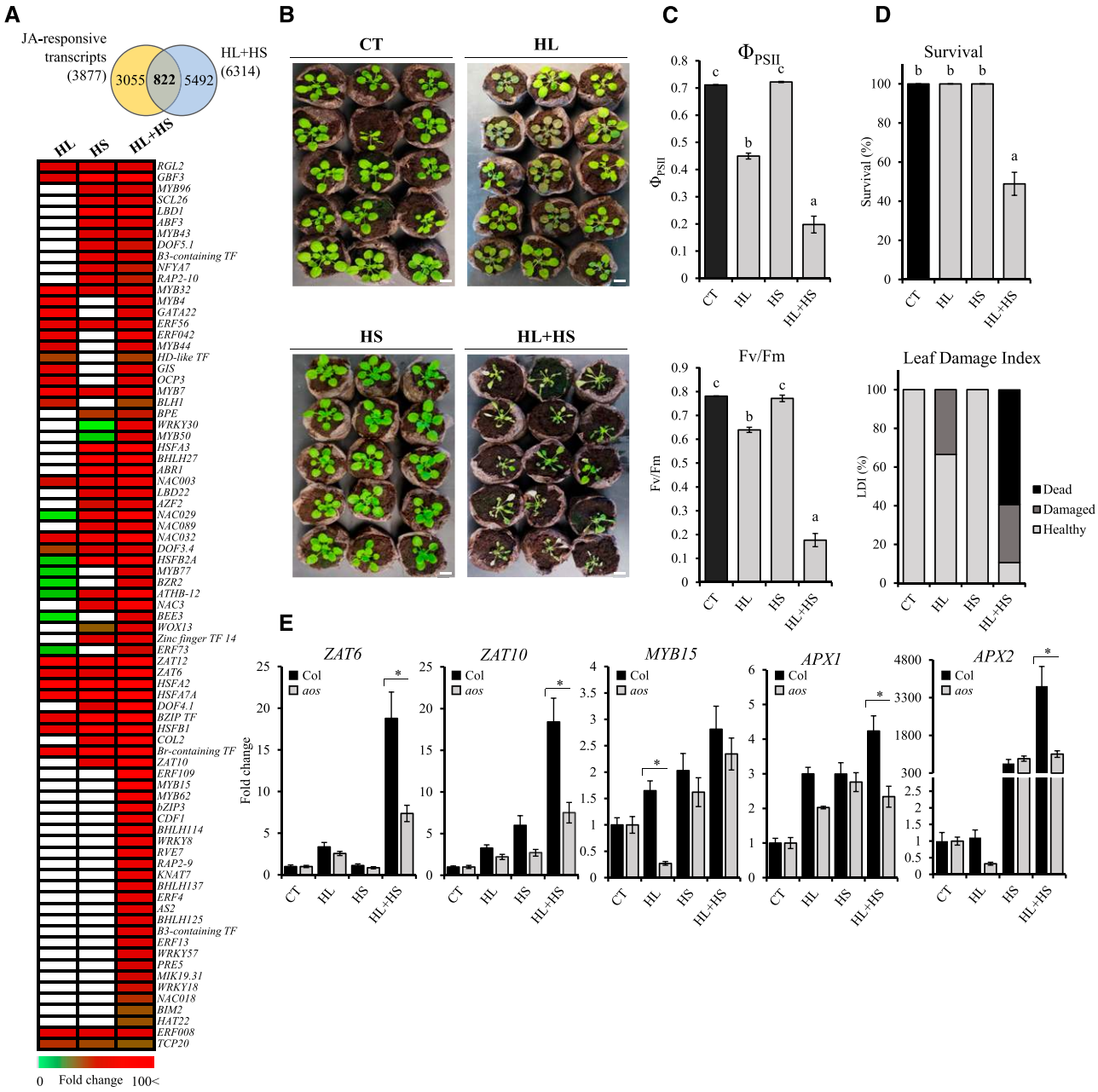

Figure 8. Involvement of JA in the response of plants to combined HL+HS. A, Venn diagram showing the overlap between JA-responsive transcripts and transcripts upregulated in response to combined HL+HS (top), and heat map showing changes in the expression of JA-response transcriptional regulators during HL, HS, and HL+HS (bottom). B, Representative images of *aos* plants subjected to the different stress treatments. Scale bar = 1 cm. C, Φ_{PSII} (top) and F_v/F_m (bottom) immediately after the application of each stress in *aos* plants. D, LDI showing the appearance of *aos* plants in response to each stress treatment (top) and survival of *aos* plants subjected to the different stress treatments (bottom). Values statistically different at $P < 0.05$ are denoted with different letters. E, Relative expression of the transcriptional regulators *ZAT6*, *ZAT10*, and *MYB15* and the ROS-scavengers *APX1* and *APX2* in Col and *aos* plants in response to the different stresses. Error bars represent SD ($n = 30$). Asterisks denote Student's *t* test significance at $P < 0.05$.

exact molecular mechanisms that control such interesting interactions.

Expression analysis of transcripts encoding different photosynthetic proteins, as well as proteins involved in the degradation, repair, and reassembly of PSII (Fig. 5, A and C; Lu, 2016), suggested that during combined HL and HS, the de novo biosynthesis of many proteins comprising the photosynthetic apparatus (e.g. PsbA [D1], PsbD [D2], PsbC [CP43], and PsbB [CP47]; Fig. 5A) is enhanced. Nevertheless, the steady-state

Table 2. *Survival rate (%), LDI (%), and photosynthetic parameters (Φ_{PSII} and F_v/F_m) of Col,* aos, sid2, *and* aba2 *mutants subjected to combined HL+HS*

Data were taken from Figures 1 and 8, and Supplemental Figs. S6 and S7. Values are means ± SD. Asterisks denote statistical significance at $P < 0.05$ (ANOVA) with respect to that in Col.

Parameter	Col	*aos*	*sid2*	*aba2*
Survival (%)	75.0 ± 5.0	48.9 ± 5.8*	75.5 ± 5.9	77.7 ± 4.4
Leaf damage index (%)				
Dead	34.9 ± 7.8	60.1 ± 6.5*	41.8 ± 13.3	37.6 ± 8.9
Damaged	38.2 ± 7.6	30.0 ± 4.1	33.3 ± 6.8	35.7 ± 2.5
Healthy	26.9 ± 5.9	9.9 ± 3.0*	24.9 ± 9.1	26.7 ± 8.1
Φ_{PSII}	0.19 ± 0.05	0.20 ± 0.03	0.11 ± 0.03	0.19 ± 0.04
F_v/F_m	0.22 ± 0.04	0.18 ± 0.02	0.14 ± 0.02	0.18 ± 0.04

level of the D1 protein declined during HL+HS stress combination (Fig. 5B; Supplemental Fig. S3A), suggesting that the rate of photodamage to PSII occurring during this stress combination (Fig. 1, B and C) exceeds the active biosynthesis, repair, and reassembly of D1 proteins (Fig. 5, A and C). As a possible consequence, PSII activity and plant survival would decline during combined HL and HS (Fig. 1). Further studies directly measuring the rate of D1 turnover are of course needed to address this possibility. Because HS and HL+HS result in enhanced accumulation of ROS (Fig. 7A), and ROS were proposed to directly or indirectly affect the rate of D1 turnover (Murata et al., 2007; Yamamoto et al., 2008), the role of ROS in affecting PSII function during HL+HS combination should also be addressed in future studies. In contrast to HL+HS, D1 protein markedly accumulated under HL (Fig. 5B) and the HL-induced decrease in PSII activity could be restored 24 h after the stress period (Fig. 1), probably due to the induction of D1 turnover and PSII repair and assembly (Fig. 5C; Bailey et al., 2002). In this respect it should be noted that only HL specifically induces the expression of transcripts encoding MPH2, a chloroplast thylakoid lumen protein that is required for proper photosynthetic acclimation of plants under fluctuating light environments (Fig. 5C; Liu and Last, 2017).

Whereas we did not observe a significant change in the acclimation response of ABA- and SA-deficient mutants (*aba2* and *sid2*, respectively) to HL+HS (compared to wild-type Col; Table 2; Supplemental Figs. S6 and S7), we found a significant decline in the ability of the JA biosynthesis mutant *aos* to acclimate to a combination of HL+HS (Fig. 8; Table 2). The AOS protein produces most of the nonvolatile oxylipins in plants and is a focus of attention in large part due to its key role in the biosynthesis of JA and biologically active JA-Ile (Farmer and Goossens, 2019). Although JA and JA-Ile have been widely associated with the defense response of plants against pathogens and insect attack (Wasternack, 2015), many of the roles of jasmonates in nature are still unknown (Hickman et al., 2017; Farmer and Goossens, 2019). Our findings suggest that JA-dependent gene expression could be important for plant acclimation to combined HL+HS (Fig. 8). For instance, expression of the JA-regulated *ZAT6* (Suzuki et al., 2015; Hickman et al., 2017) and the ROS- (Willems et al., 2016) and OPDA-regulated *ZAT10* (Taki et al., 2005), or the ROS- and redox-regulated scavengers *APX1* and *APX2* (all important transcripts involved in the acclimation of plants to different abiotic stresses) was significantly reduced in response to HL+HS in *aos* plants compared to Col (Fig. 8E). *ZAT6* is proposed to positively modulate biotic and abiotic stress tolerance (Shi et al., 2014) as well as cadmium tolerance through a glutathione-dependent pathway (Chen et al., 2016). *ZAT10* is involved in *APX2* induction in response to excess light (Li et al., 2009) and overexpression of *ZAT10* results in enhanced tolerance to photoinhibitory light (Rossel et al., 2007) as well as enhanced tolerance to salinity, heat, and osmotic stresses in Arabidopsis plants (Mittler et al., 2006). Interestingly, *ZAT10* expression was reported to be OPDA-dependent (Taki et al., 2005), suggesting that the elevated OPDA levels observed in Col plants subjected to HL+HS (Fig. 7D) could contribute, in combination with other factors such as redox and/or ROS, to the enhanced expression of *ZAT10* during combined HL+HS. *APX1* plays an important role in Arabidopsis tolerance to the combination of drought and HS (Koussevitzky et al., 2008; Zandalinas et al., 2016a). In addition, it has been reported that *APX2* is induced by HL intensities and HS (Panchuk et al., 2002; Mullineaux et al., 2006), and that the induction of *APX2* by excess light involved H_2O_2 (accumulated in response to HS and HL+HS; Fig. 7; Fryer et al., 2003; Rossel et al., 2006; Bechtold et al., 2008). The JA-dependent modulation of these transcripts in response to the combination of HL and HS could therefore be important for plant acclimation to a combination of HL+HS. Further studies are needed to shed more light on the role of each of these genes in the JA-dependent response of plants to combined HL+HS.

In nature, photosynthetic organisms may experience extreme changes in light intensity that are often accompanied by high temperatures. Taken together, our study reveals that a combination of HL and HS could dramatically compromise the photosynthetic capacity of plants, and that the plant hormone JA positively regulates plant responses to this stress combination.

MATERIALS AND METHODS

Plant Material and Growth Conditions

Arabidopsis (*Arabidopsis thaliana*) Col-0 (var Columbia-0), *aos* (Salk_01775C), *sid2* (Salk_093400C), and *aba2* (CS3835) plants were grown in peat pellets (Jiffy-7; http://www.jiffygroup.com/) at 23°C under long-day growth conditions (12-h light from 7 AM to 7 PM; 50 μmol m^{-2} s^{-1}/12-h dark from 7 PM to 7 AM).

Stress Treatments

Three different stress treatments were performed in parallel: HL, HS, and combined HL+HS (Supplemental Fig. S1). HL was applied by exposing 30-d–old plants to 600 μmol m^{-2} s^{-1} (F54T5/TL84/HO/ALTO; Philips) at 23°C for 7 h. HS was imposed by transferring 30-d–old plants to 42°C, 50 μmol m^{-2} s^{-1}, for 7 h. HL+HS was performed by simultaneously subjecting plants to 600 μmol m^{-2} s^{-1} light and 42°C for 7 h (Supplemental Fig. S1). CT plants were maintained at 50 μmol m^{-2} s^{-1}, 23°C. After the stress treatments, plants of each treatment were divided into those plants sampled for analysis described in Supplemental Figure S1, and those plants that were allowed to recover under controlled conditions until flowering time to score for survival. Twenty-four hours after the stress treatments, LDI (Gallas and Waters, 2015) and PSII activity (Φ_{PSII}, F_v/F_m) were also determined (Supplemental Fig. S1). All experiments were carried out at the same time of the light cycle (from 9 AM to 4 PM) and were repeated at least three times.

Photosynthetic Parameters

Φ_{PSII} and F_v/F_m were measured using a portable fluorometer (model no. 110/S FluorPen; Photon Systems Instruments). Photosynthetic parameters were analyzed at two time points: immediately after the 7 h of individual and combined stress treatments, and 24 h after the stress treatments (recovery; Supplemental Fig. S1). Photosynthetic measurements were taken for at least 15 plants using two fully expanded young leaves per plant for each stress treatment, and each experiment was repeated at least three times.

Stomatal Aperture Measurements and Leaf Temperatures

Stomatal aperture analyses were performed as described by Morillon and Chrispeels (2001) and Zandalinas et al., (2016a). Briefly, two leaves per plant were cut and their lower surface was immediately stuck to a microspore slide with a medical adhesive (Hollister). The leaf was removed and the slides were washed with distilled water. The lower epidermis of the leaf stuck to the slide was visualized under the microscope and stomatal images acquired. Measurements of stomatal aperture were performed with the imaging software ImageJ (https://imagej.net/). At least 600 stomata were measured in 15 plants for each treatment. Surface leaf temperature was measured using an infrared thermal camera (FLIR C2; Flir Systems, https://www.flir.com/). Leaf temperature was measured on two expanded young leaves per plant using at least 15 plants for each stress treatment.

RWC

Rosette RWC was calculated at the end of the stress treatments. Rosettes were weighed to obtain a fresh mass (M_f) immediately after the individual and combined stresses. Rosettes were allowed to rehydrate overnight in an opaque beaker filled with distilled water. Then, they were reweighed to obtain turgid mass (M_t). Finally, rosettes were dried at 80°C for 48 h to obtain dry mass (M_d). RWC was calculated as $\left[\left(M_f - M_d\right)/\left(M_t - M_d\right)\right] \times 100$ according to Morgan (1984).

RNA-Seq Analysis

Three true leaves pooled from at least 30 different plants subjected to each of the CT and stress treatments were used for each biological repeat for RNA-seq analysis, and three biological repeats were performed. Total RNA was isolated using TRIzol reagent (Invitrogen Life Technologies) according to the manufacturer's instructions and purified using a NucleoSpin RNA Clean-up Kit (Macherey-Nagel). Initial RNA sample quality, RNA quantification, preparation of RNA libraries, and sequencing were performed as described previously by Zandalinas et al. (2019a). RNA library construction and sequencing were performed by the DNA Core Facility at the University of Missouri. Single-end sequenced reads obtained from the Next-Seq 500 (Illumina) platform were quality-tested using the program FastQC v0.11.7 (https://www.bioinformatics.babraham.ac.uk/projects/fastqc/) and aligned to the reference genome of Arabidopsis (Genome Build 10) obtained from The Arabidopsis Information Resource (https://www.arabidopsis.org/) using STAR Aligner v2.4.0.1 (Dobin et al., 2013). Default mapping parameters (10 mismatches/read; nine multimapping locations/read) were used as described in Zandalinas et al. (2019a). The genome index was generated using the gene annotation file (gff file) obtained from The Arabidopsis Information Resource (https://www.arabidopsis.org/) for Genome Build 10. Differential gene expression analysis was carried out using the R-based package DESeq2 v1.20.0 that is available in Bioconductor (Love et al., 2014). Transcripts differentially expressed compared to CTs were identified by examining the difference in their abundance under the different conditions. The difference in expression was quantified in terms of the logarithm of the ratio of mean normalized counts between two conditions (log fold change) and differentially expressed transcripts were defined as those with an adjusted P value < 0.05 in their fold change (negative binomial Wald test followed by a Benjamini–Hochberg correction). Functional annotations and overrepresentation of GO terms ($P < 0.05$) were performed using the program DAVID Bioinformatics Resources 6.8 (https://david.ncifcrf.gov/; Huang et al., 2009). Heat maps were generated using the software MeV v. 4.9.0 (Saeed et al., 2006).

TEM

Leaves of Col plants subjected to the different stress treatments were analyzed by TEM as described in Zandalinas et al. (2019b). Briefly, leaves were fixed in 2% (w/v) paraformaldehyde and 2% (w/v) glutaraldehyde in 100 mM of sodium cacodylate buffer at pH 7.35. Fixed tissues were rinsed with 100 mM of sodium cacodylate buffer at pH 7.35 containing 130 mM of Suc. Secondary fixation was performed using 1% (w/v) osmium tetroxide (Ted Pella) in cacodylate buffer using a Pelco Biowave (Ted Pella) operated at 100 W for 1 min. Tissues were incubated at 4°C for 1 h, then rinsed with cacodylate buffer followed by washes with distilled water. En bloc staining was performed using 1% (w/v) aqueous uranyl acetate, incubated at 4°C overnight and then rinsed with distilled water. A graded dehydration series was performed using ethanol which was transitioned into acetone, and dehydrated tissues were then infiltrated with a 1:1 v/v of Epon and Spurr resin for 24 h at room temperature and polymerized at 60°C overnight. Sections were cut to a thickness of 80 nm using an Ultracut UCT Ultramicrotome (Leica Microsystems) and a diamond knife (Diatome). Images were acquired with a model no. JEM 1400 TEM (JEOL) at 80 kV on a model no. Ultrascan 1000 charge-coupled device camera (Gatan) at the Electron Microscopy Core Facility, University of Missouri. At least 100 images, each containing two to four chloroplasts from at least three different plants from each treatment, were analyzed. Affected starch granules were defined as those containing black spots/lines and the number of thylakoids was recorded per 1 μm perpendicular to thylakoid orientation in at least 50 chloroplasts per stress treatment.

H_2O_2 and Hormonal Analysis

Hormone extraction and analysis were carried out as described in Durgbanshi et al. (2005) with a few modifications. Briefly, before hormonal extraction, a mixture containing 50 ng of [$^2H_6$]-ABA, [C_{13}]-SA, and dihydrojasmonic acid was added to 0.1 g of dry tissue. The tissue was immediately homogenized in 2 mL of ultrapure water in a ball mill (MillMix20; Domel). After centrifugation at 4,000g, 4°C, for 10 min, supernatants were recovered and pH-adjusted to "3" with 30% (v/v) acetic acid. The water extract was partitioned twice against 2 mL of diethyl ether and the organic layer recovered and evaporated under vacuum in a centrifuge concentrator (Speed Vac; Jouan). Once dried, the residue was resuspended in a 10:90 MeOH:H_2O solution by gentle sonication. The resulting solution was filtered through 0.22-μm polytetrafluoroethylene membrane syringe filters (Albet) and directly injected into an ultra-performance LC system (Acquity SDS; Waters). Chromatographic separations were carried out on a reversed-phase C18 column (gravity, 50 × 2.1 mm, 1.8-μm particle size; Macherey-Nagel) using a MeOH:H_2O (both supplemented with 0.1% [v/v] acetic acid) gradient at a flow rate of 300 μL min^{-1}. Hormones were quantified with a TQ-S Triple Quadrupole Mass Spectrometer (Micromass). A standard curve consisting of 0, 1, 2, 4, 8, 16, 30, 62, and 100 μg L^{-1} of JA, OPDA, and JA-Ile was used to quantify each compound.

H_2O_2 accumulation in leaves was measured using the Amplex Red Hydrogen Peroxide-Peroxidase Assay kit (Molecular Probes/Invitrogen) as described in Suzuki et al. (2015) and Zandalinas et al. (2016a). Briefly, 500 μL of 50-mM sodium P buffer at pH 7.4, containing 50-μM Amplex Red and 0.05 U mL^{-1} horseradish peroxidase, was added to ground, frozen tissues. Samples were centrifuged at 12,000*g* for 12 min at 4°C. A quantity of 450 μL of supernatant was transferred into fresh tubes and incubated for 30 min at room temperature in the dark. Absorbance at 560 nm was measured using a NanoDrop Spectrophotometer (Thermo Fisher Scientific). The concentration of H_2O_2 in each sample was determined from a standard curve consisting of 0, 0.5, 1, 3, 6, and 9 μM of H_2O_2. After absorbance measurement, tissue samples were dried using a speed vacuum concentrator for 90 min and H_2O_2 accumulation per gram of dry weight was calculated.

Immunoblot and Reverse Transcription Quantitative PCR Analysis

Protein was isolated, quantified, and analyzed via immunoblots as described by Zandalinas et al. (2016a). Relative expression analysis by reverse transcription quantitative PCR (RT-qPCR) was performed according to Zandalinas et al. (2016b) by using the CFX Connect Real-Time PCR Detection System (Bio-Rad) and gene-specific primers (Supplemental Table S7).

Statistical Analysis

Results are presented as the mean ± SD. Statistical analysis were performed by two-way ANOVA followed by a Tukey post hoc test ($P < 0.05$) when a significant difference was detected (values at $P < 0.05$ are denoted with different letters). Differentially expressed transcripts were defined as those that had a fold change with an adjusted P value < 0.05 (ANOVA, and/or negative binomial Wald test followed by a Benjamini–Hochberg correction). Venn diagram overlaps was subjected to hypergeometric testing using the software phyper (R package; https://stat.ethz.ch/R-manual/R-devel/library/stats/html/Hypergeometric.html). For relative expression analysis by RT-qPCR, statistical analyses were performed by two-tailed Student's t test (asterisks denote statistical significance at $P < 0.05$ with respect to the wild type).

Accession Numbers

Raw and processed RNA-Seq data files were deposited in GEO (https://www.ncbi.nlm.nih.gov/geo/) under the following accession number GSE134391. PsbA (ATCG00020), ZAT6 (AT5G04340), ZAT10 (AT1G27730), APX1 (AT1G07890), APX2 (AT1G07890), MYB15 (AT3G23250). Additional accession numbers can be found in Supplemental Tables S1–S6.

Supplemental Data

The following supplemental materials are available.

Supplemental Figure S1. The experimental design used for the study of HL, HS, and combined HL+HS using Arabidopsis plants.

Supplemental Figure S2. GO annotation of transcripts specifically upregulated (top) and downregulated (bottom) in leaves of Col plants subjected to HL, HS, and combined HL+HS.

Supplemental Figure S3. Accumulation of D1 and PsaH in Col plants subjected to HL, HS, and combined HL+HS.

Supplemental Figure S4. Heat maps showing significantly upregulated and downregulated transcripts involved in JA biosynthesis and signaling in Col plants subjected to HL, HS, and combined HL+HS.

Supplemental Figure S5. PSII performance and RWC of JA-deficient *aos* plants subjected to HL, HS, and combined HL+HS.

Supplemental Figure S6. PSII performance, survival rate, LDI, RWC, and stomatal responses rate of SA-deficient *sid2* plants subjected to HL, HS, and combined HL+HS.

Supplemental Figure S7. PSII performance, survival rate, LDI, RWC, and stomatal responses rate of ABA-deficient *aba2* plants subjected to HL, HS, and combined HL+HS.

Supplemental Table S1. Transcripts significantly upregulated ($P < 0.05$) in Col plants subjected to HL.

Supplemental Table S2. Transcripts significantly upregulated ($P < 0.05$) in Col plants subjected to HS.

Supplemental Table S3. Transcripts significantly upregulated ($P < 0.05$) in Col plants subjected to the combination of HL+HS.

Supplemental Table S4. Transcripts significantly downregulated ($P < 0.05$) in Col plants subjected to HL.

Supplemental Table S5. Transcripts significantly downregulated ($P < 0.05$) in Col plants subjected to HS.

Supplemental Table S6. Transcripts significantly downregulated ($P < 0.05$) in Col plants subjected to the combination of HL+HS.

Supplemental Table S7. Transcript-specific primers used for relative expression analysis by RT-qPCR.

ACKNOWLEDGMENTS

We thank the University of Missouri DNA Core Facility for providing the RNAseq service and the University of Missouri Electron Microscopy Core for providing electron microscopy services. Hormone measurements were carried out at the central facilities (Servei Central d'Instrumentació Científica) of the Universitat Jaume I. We thank Dr. Rachel Nechushtai for the gift of D1 and PsaH antibodies.

Received August 2, 2019; accepted September 27, 2019; published October 8, 2019.

LITERATURE CITED

Allen JF, de Paula WBM, Puthiyaveetil S, Nield J (2011) A structural phylogenetic map for chloroplast photosynthesis. Trends Plant Sci **16:** 645–655

Baena-González E, Aro E-M (2002) Biogenesis, assembly and turnover of photosystem II units. Philos Trans R Soc Lond B Biol Sci **357:** 1451–1459, discussion 1459–1460

Bailey S, Thompson E, Nixon PJ, Horton P, Mullineaux CW, Robinson C, Mann NH (2002) A critical role for the Var2 FtsH homologue of *Arabidopsis thaliana* in the photosystem II repair cycle in vivo. J Biol Chem **277:** 2006–2011

Bechtold U, Richard O, Zamboni A, Gapper C, Geisler M, Pogson B, Karpinski S, Mullineaux PM (2008) Impact of chloroplastic- and extracellular-sourced ROS on high light-responsive gene expression in Arabidopsis. J Exp Bot **59:** 121–133

Bondada BR, Syvertsen JP (2005) Concurrent changes in net CO_2 assimilation and chloroplast ultrastructure in nitrogen deficient citrus leaves. Environ Exp Bot **54:** 41–48

Chehab EW, Kim S, Savchenko T, Kliebenstein D, Dehesh K, Braam J (2011) Intronic T-DNA insertion renders Arabidopsis opr3 a conditional jasmonic acid-producing mutant. Plant Physiol **156:** 770–778

Chehab EW, Yao C, Henderson Z, Kim S, Braam J (2012) Arabidopsis touch-induced morphogenesis is jasmonate mediated and protects against pests. Curr Biol **22:** 701–706

Chen J, Yang L, Yan X, Liu Y, Wang R, Fan T, Ren Y, Tang X, Xiao F, Liu Y, et al (2016) Zinc-finger transcription factor ZAT6 positively regulates cadmium tolerance through the glutathione-dependent pathway in Arabidopsis. Plant Physiol **171:** 707–719

Choudhury FK, Rivero RM, Blumwald E, Mittler R (2017) Reactive oxygen species, abiotic stress and stress combination. Plant J **90:** 856–867

Dar TA, Uddin M, Khan MMA, Hakeem KR, Jaleel H (2015) Jasmonates counter plant stress: A review. Environ Exp Bot **115:** 49–57

Devireddy AR, Zandalinas SI, Gómez-Cadenas A, Blumwald E, Mittler R (2018) Coordinating the overall stomatal response of plants: Rapid leaf-to-leaf communication during light stress. Sci Signal **11:** 518

Dobin A, Davis CA, Schlesinger F, Drenkow J, Zaleski C, Jha S, Batut P, Chaisson M, Gingeras TR (2013) STAR: Ultrafast universal RNA-seq aligner. Bioinformatics **29:** 15–21

Dogra V, Duan J, Lee KP, Kim C (2019) Impaired PSII proteostasis triggers a UPR-like response in the var2 mutant of Arabidopsis. J Exp Bot **70:** 3075–3088

Durgbanshi A, Arbona V, Pozo O, Miersch O, Sancho JV, Gómez-Cadenas A (2005) Simultaneous determination of multiple phytohormones in plant extracts by liquid chromatography–electrospray tandem mass spectrometry. J Agric Food Chem **53:** 8437–8442

Edelman M, Mattoo AK (2008) D1-protein dynamics in photosystem II: The lingering enigma. Photosynth Res **98:** 609–620

Farmer EE, Goossens A (2019) Jasmonates: What ALLENE OXIDE SYNTHASE does for plants. J Exp Bot **70:** 3373–3378

Flexas J, Bota J, Escalona JM, Sampol B, Medrano H (2002) Effects of drought on photosynthesis in grapevines under field conditions: An evaluation of stomatal and mesophyll limitations. Funct Plant Biol **29:** 461–471

Fryer MJ, Ball L, Oxborough K, Karpinski S, Mullineaux PM, Baker NR (2003) Control of Ascorbate Peroxidase 2 expression by hydrogen peroxide and leaf water status during excess light stress reveals a functional organisation of Arabidopsis leaves. Plant J **33:** 691–705

Gallas G, Waters ER (2015) Boechera species exhibit species-specific responses to combined heat and high light stress. PLoS One **10:** e0129041

Gasperini D, Chételat A, Acosta IF, Goossens J, Pauwels L, Goossens A, Dreos R, Alfonso E, Farmer EE (2015) Multilayered organization of jasmonate signalling in the regulation of root growth. PLoS Genet **11:** e1005300

Hewezi T, Léger M, Gentzbittel L (2008) A comprehensive analysis of the combined effects of high light and high temperature stresses on gene expression in sunflower. Ann Bot **102:** 127–140

Hickman R, Van Verk MC, Van Dijken AJH, Mendes MP, Vroegop-Vos IA, Caarls L, Steenbergen M, Van der Nagel I, Wesselink GJ, Jironkin A, et al (2017) Architecture and dynamics of the jasmonic acid gene regulatory network. Plant Cell **29:** 2086–2105

Hu Y, Jiang L, Wang F, Yu D (2013) Jasmonate regulates the inducer of cbf expression-C-repeat binding factor/DRE binding factor1 cascade and freezing tolerance in Arabidopsis. Plant Cell **25:** 2907–2924

Huang W, Sherman BT, Lempicki RA (2009) Systematic and integrative analysis of large gene lists using DAVID bioinformatics resources. Nat Protoc **4:** 44–57

Järvi S, Suorsa M, Aro E-M (2015) Photosystem II repair in plant chloroplasts—Regulation, assisting proteins and shared components with photosystem II biogenesis. Biochim Biophys Acta **1847:** 900–909

Kazan K (2015) Diverse roles of jasmonates and ethylene in abiotic stress tolerance. Trends Plant Sci **20:** 219–229

Koussevitzky S, Suzuki N, Huntington S, Armijo L, Sha W, Cortes D, Shulaev V, Mittler R (2008) Ascorbate peroxidase 1 plays a key role in the response of *Arabidopsis thaliana* to stress combination. J Biol Chem **283:** 34197–34203

Li Z, Wakao S, Fischer BB, Niyogi KK (2009) Sensing and responding to excess light. Annu Rev Plant Biol **60:** 239–260

Liu J, Last RL (2017) A chloroplast thylakoid lumen protein is required for proper photosynthetic acclimation of plants under fluctuating light environments. Proc Natl Acad Sci USA **114:** E8110–E8117

Love MI, Huber W, Anders S (2014) Moderated estimation of fold change and dispersion for RNA-seq data with DESeq2. Genome Biol **15:** 550

Lu Y (2016) Identification and roles of photosystem II assembly, stability, and repair factors in Arabidopsis. Front Plant Sci **7:** 168

Mathur S, Agrawal D, Jajoo A (2014) Photosynthesis: Response to high temperature stress. J Photochem Photobiol B **137:** 116–126

Mittler R (2006) Abiotic stress, the field environment and stress combination. Trends Plant Sci **11:** 15–19

Mittler R, Kim Y, Song L, Coutu J, Coutu A, Ciftci-Yilmaz S, Lee H, Stevenson B, Zhu J-K (2006) Gain- and loss-of-function mutations in Zat10 enhance the tolerance of plants to abiotic stress. FEBS Lett **580:** 6537–6542

Morgan JA (1984) Interaction of water supply and N in wheat. Plant Physiol **76:** 112–117

Morillon R, Chrispeels MJ (2001) The role of ABA and the transpiration stream in the regulation of the osmotic water permeability of leaf cells. Proc Natl Acad Sci USA **98:** 14138–14143

Mullineaux PM, Karpinski S, Baker NR (2006) Spatial dependence for hydrogen peroxide-directed signaling in light-stressed plants. Plant Physiol **141:** 346–350

Murata N, Takahashi S, Nishiyama Y, Allakhverdiev SI (2007) Photoinhibition of photosystem II under environmental stress. Biochim Biophys Acta **1767:** 414–421

Nishiyama Y, Allakhverdiev SI, Murata N (2006) A new paradigm for the action of reactive oxygen species in the photoinhibition of photosystem II. Biochim Biophys Acta **1757:** 742–749

Ort DR (2001) When there is too much light. Plant Physiol **125:** 29–32

Panchuk II, Volkov RA, Schöffl F (2002) Heat stress- and heat shock transcription factor-dependent expression and activity of ascorbate peroxidase in Arabidopsis. Plant Physiol **129:** 838–853

Park J-H, Halitschke R, Kim HB, Baldwin IT, Feldmann KA, Feyereisen R (2002) A knock-out mutation in allene oxide synthase results in male sterility and defective wound signal transduction in Arabidopsis due to a block in jasmonic acid biosynthesis. Plant J **31:** 1–12

Peleg Z, Blumwald E (2011) Hormone balance and abiotic stress tolerance in crop plants. Curr Opin Plant Biol **14:** 290–295

Pospíšil P (2016) Production of reactive oxygen species by photosystem II as a response to light and temperature stress. Front Plant Sci **7:** 1950

Rizhsky L, Liang H, Mittler R (2002) The combined effect of drought stress and heat shock on gene expression in tobacco. Plant Physiol **130:** 1143–1151

Rizhsky L, Liang H, Shuman J, Shulaev V, Davletova S, Mittler R (2004) When defense pathways collide. The response of Arabidopsis to a combination of drought and heat stress. Plant Physiol **134:** 1683–1696

Rossel JB, Walter PB, Hendrickson L, Chow WS, Poole A, Mullineaux PM, Pogson BJ (2006) A mutation affecting ASCORBATE PEROXIDASE 2 gene expression reveals a link between responses to high light and drought tolerance. Plant Cell Environ **29:** 269–281

Rossel JB, Wilson PB, Hussain D, Woo NS, Gordon MJ, Mewett OP, Howell KA, Whelan J, Kazan K, Pogson BJ (2007) Systemic and intracellular responses to photooxidative stress in Arabidopsis. Plant Cell **19:** 4091–4110

Ruban AV (2015) Evolution under the sun: Optimizing light harvesting in photosynthesis. J Exp Bot **66:** 7–23

Ruban AV (2009) Plants in light. Commun Integr Biol **2:** 50–55

Saeed AI, Bhagabati NK, Braisted JC, Liang W, Sharov V, Howe EA, Li J, Thiagarajan M, White JA, Quackenbush J (2006) TM4 microarray software suite. Methods Enzymol **411:** 134–193

Shi H, Wang X, Ye T, Chen F, Deng J, Yang P, Zhang Y, Chan Z (2014) The cysteine2/histidine2-type transcription factor ZINC FINGER OF ARABIDOPSIS THALIANA6 modulates biotic and abiotic stress responses by activating salicylic acid-related genes and C-REPEAT-BINDING FACTOR genes in Arabidopsis. Plant Physiol **165:** 1367–1379

Song L, Huang SC, Wise A, Castanon R, Nery JR, Chen H, Watanabe M, Thomas J, Bar-Joseph Z, Ecker JR (2016) A transcription factor hierarchy defines an environmental stress response network. Science **354:** aag1550

Spicher L, Almeida J, Gutbrod K, Pipitone R, Dörmann P, Glauser G, Rossi M, Kessler F (2017) Essential role for phytol kinase and tocopherol in tolerance to combined light and temperature stress in tomato. J Exp Bot **68:** 5845–5856

Stenzel I, Hause B, Miersch O, Kurz T, Maucher H, Weichert H, Ziegler J, Feussner I, Wasternack C (2003) Jasmonate biosynthesis and the allene oxide cyclase family of *Arabidopsis thaliana*. Plant Mol Biol **51:** 895–911

Su X, Wu S, Yang L, Xue R, Li H, Wang Y, Zhao H (2014) Exogenous progesterone alleviates heat and high light stress-induced inactivation of photosystem II in wheat by enhancing antioxidant defense and D1 protein stability. Plant Growth Regul **74:** 311–318

Suzuki N, Devireddy AR, Inupakutika MA, Baxter A, Miller G, Song L, Shulaev E, Azad RK, Shulaev V, Mittler R (2015) Ultra-fast alterations in mRNA levels uncover multiple players in light stress acclimation in plants. Plant J **84:** 760–772

Suzuki N, Rivero RM, Shulaev V, Blumwald E, Mittler R (2014) Abiotic and biotic stress combinations. New Phytol **203:** 32–43

Szymańska R, Ślesak I, Orzechowska A, Kruk J (2017) Physiological and biochemical responses to high light and temperature stress in plants. Environ Exp Bot **139:** 165–177

Takahashi S, Murata N (2008) How do environmental stresses accelerate photoinhibition? Trends Plant Sci **13:** 178–182

Taki N, Sasaki-Sekimoto Y, Obayashi T, Kikuta A, Kobayashi K, Ainai T, Yagi K, Sakurai N, Suzuki H, Masuda T, et al (2005) 12-oxo-phytodienoic acid triggers expression of a distinct set of genes and plays a role

in wound-induced gene expression in Arabidopsis. Plant Physiol **139:** 1268–1283

Teskey R, Wertin T, Bauweraerts I, Ameye M, McGuire MA, Steppe K (2015) Responses of tree species to heat waves and extreme heat events. Plant Cell Environ **38:** 1699–1712

Urban J, Ingwers MW, McGuire MA, Teskey RO (2017) Increase in leaf temperature opens stomata and decouples net photosynthesis from stomatal conductance in *Pinus taeda* and *Populus deltoides* × *nigra*. J Exp Bot **68:** 1757–1767

Wasternack C (2015) How jasmonates earned their laurels: Past and present. J Plant Growth Regul **34:** 761–794

Wasternack C, Hause B (2013) Jasmonates: Biosynthesis, perception, signal transduction and action in plant stress response, growth and development. An update to the 2007 review in *Annals of Botany*. Ann Bot **111:** 1021–1058

Willems P, Mhamdi A, Stael S, Storme V, Kerchev P, Noctor G, Gevaert K, Van Breusegem F (2016) The ROS wheel: Refining ROS transcriptional footprints. Plant Physiol **171:** 1720–1733

Yamamoto Y, Aminaka R, Yoshioka M, Khatoon M, Komayama K, Takenaka D, Yamashita A, Nijo N, Inagawa K, Morita N, et al (2008) Quality control of photosystem II: Impact of light and heat stresses. Photosynth Res **98:** 589–608

Zandalinas SI, Balfagón D, Arbona V, Gómez-Cadenas A, Inupakutika MA, Mittler R (2016a) ABA is required for the accumulation of APX1 and MBF1c during a combination of water deficit and heat stress. J Exp Bot **67:** 5381–5390

Zandalinas SI, Rivero RM, Martínez V, Gómez-Cadenas A, Arbona V (2016b) Tolerance of citrus plants to the combination of high temperatures and drought is associated to the increase in transpiration modulated by a reduction in abscisic acid levels. BMC Plant Biol **16:** 105

Zandalinas SI, Sengupta S, Burks D, Azad RK, Mittler R (2019a) Identification and characterization of a core set of ROS wave-associated transcripts involved in the systemic acquired acclimation response of Arabidopsis to excess light. Plant J **98:** 126–141

Zandalinas SI, Song L, Sengupta S, McInturf S, Grant DG, Marjault H-B, Castro-Guerrero NA, Burks D, Azad RK, Mendoza-Cozatl DG, et al (2019b) Expression of a dominant-negative AtNEET-H89C protein disrupts iron-sulfur metabolism and iron homeostasis in Arabidopsis. Plant J doi:10.1111/TPJ.14581